JOC Article

DFT Calculations on the Protonation of Two 1,3-Butadiyne Units Fixed in Medium-Sized Rings

Birgit Esser and Rolf Gleiter*

Organisch-Chemisches Institut der Universität Heidelberg, Im Neuenheimer Feld 270, D-69120 Heidelberg, Germany

rolf.gleiter@oci.uni-heidelberg.de

Received February 28, 2006

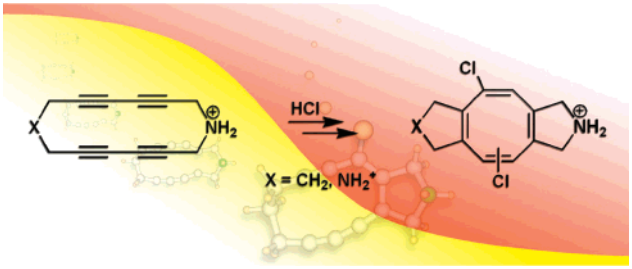

The *N*-bis-protonated forms of 1-azacyclotetradeca-3,5,10,12-tetrayne (**19**) and 1,8-diazacyclotetradeca-3,5,10,12-tetrayne (**20**) were used as model systems to study the HCl addition to two 1,3-butadiyne units in close proximity using quantum chemical means. The model calculations were carried out mainly at the B3LYP/3-21G or 6-31G* level. The basis set 6-311G* was used for single-point calculations. The calculations reveal that **19** and **20** are preferably protonated at the C4 center accompanied by a transannular ring closure between C3 and C13 yielding the bicyclic systems **23** and **24**, respectively. Further stabilization of these vinyl cations is achieved by a second transannular ring closure between C6 and C10 leading to the 5−8−5 tricyclic systems **27** and **28**, which are further stabilized by the addition of a chloride anion. The different regiochemistry experimentally observed for **13b** and **16b** was rationalized by calculating local softness parameters. The observed product selectivities for the formation of **14b** and **15b** were traced back to the relative stabilities of the primary protonation products **23** and **24**, respectively. Model calculations on 1-azacyclopentadeca-3,5,11,13-tetrayne (**65**) and 1-azacyclohexa-deca-3,5,12,14-tetrayne (**66**) as examples for medium-sized rings with nonparallel 1,3-butadiyne units revealed a concerted process of protonation and C3−C15 (**65**) or C3−C16 (**66**) ring closure. The second step is the formation of an aromatic central ring as a result of a ring closure between C6−C13 and C6−C14, respectively.

Introduction

The reaction of alkynes with hydrochloric acid or the acid-catalyzed hydration of acetylenes are basic reactions of wide interest concerning the use, the mechanism, and the possible intermediates.[1] Several studies on the protonation of alkynes in solution revealed the intermediacy of a vinyl cation.[2] Kinetic studies demonstrated that the reactions of mono- or disubstituted alkynes with electrophiles proceed via an AdE2 mechanism. In the case of the HCl addition in solution, the transition state resembles the vinyl chloride ion pair **2** (Scheme 1).[3] For *o*-bis-(phenylethynyl)benzene (**4**), the reaction with electrophiles revealed a pseudo AdE3 mechanism. The triple bond, which is attacked by the electrophile (E^+), suffers AdE3 electrophilic attack, and the triple bond that serves as a nucleophile does so in an AdE2 manner[4] (see **5**). In those cases when both triple bonds are aligned parallel, such an AdE3/AdE2 situation should occur very easily. Indeed, when 1,6-diazacyclodeca-3,8-diynes (**7**) were treated with concentrated hydrochloric acid, a transannular ring closure to **9** was observed (see Scheme 2).[5] These

(1) Reviews: (a) Schmid, G. H. In *The chemistry of the carbon−carbon triple bond*; Patai, S., Ed.; J. Wiley & Sons: Chichester, 1978; pp 275−341. (b) Boyd, G. V. In *Supplement C2: The chemistry of triple bonded functional groups*; Patai, S., Ed.; J. Wiley & Sons: Chichester, 1994; pp 287−374. (c) Shostakovski, M. F.; Bogdanova, A. V. *The Chemistry of Diacetylenes*; J. Wiley & Sons: New York, 1974.

(2) (a) Noyce, D. S.; Schiavelli, M. D. *J. Am. Chem. Soc.* **1968**, *90*, 1020−1022. (b) Lucchini, V.; Modena, G. *J. Am. Chem. Soc.* **1990**, *112*, 6291−6296.

(3) Fahey, R. C.; Payne, M. T.; Lee, D.-J. *J. Org. Chem.* **1974**, *39*, 1124−1130.

(4) Whitlock, H. W.; Sandvick, P. E.; Overman, L. E.; Reichhardt, P. B. *J. Org. Chem.* **1969**, *34*, 879−886.

10.1021/jo060426h CCC: $33.50
Published on Web 06/06/2006

SCHEME 1. Proposed Mechanism for the Reaction of 1 with HCl and of 4 with an Electrophile

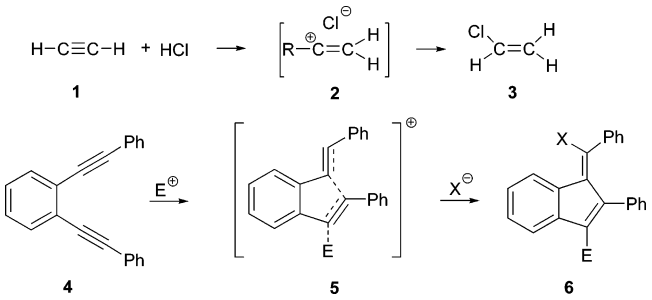

SCHEME 2. Experimental Results for the Addition of Hydrochloric Acid to 7

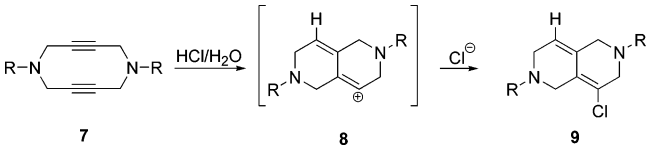

investigations led to the question of how two parallel 1,3-butadiyne units would react with electrophiles. For cycles incorporating two 1,3-butadiyne units such as 1,2:7,8-dibenzocyclododeca-1,7-dien-3,5,9,11-tetrayne (**10a**) or its tetrabutyl derivative (**10b**), reduction processes as well as the reaction with iodine (Scheme 3) revealed transannular reactions of the central moieties to a 5−6−5 tricyclic unit.[6−8]

To carry out the corresponding studies with electrophiles in aqueous medium, the two azacycles, 1-azacyclotetradeca-3,5,-10,12-tetrayne (**13**) and 1,8-diazacyclotetradeca-3,5,10,12-tetrayne (**16**; Scheme 4), were chosen. As a result of the propano bridges, they provide a higher flexibility for a ring closure and, in comparison to **7**, more possibilities for a protonation of the diyne unit (four for **13** and two for **16**).

In Scheme 4, the results of the HCl addition to **13b** and **16b** are summarized. In contrast to the reactions of the 12-membered bis(1,3-butadiyne) systems **10a** and **10b**, two different ring-closing modes were found.[9,10] To understand these modes and the observed regioselectivities, we carried out quantum chemical calculations. In particular, the following questions were tackled: What are the intermediates and transition states of the ring-closing reactions summarized in Scheme 4 and how can the observed regioselectivity and product selectivity be rationalized?

Methods of Calculation. We mainly used the density functional theory (DFT)[11] by applying the three parameter hybrid functional by Becke (B3)[12] and the correlation functionals suggested by Lee, Yang, and Parr (LYP).[13] As basis sets, we used those recommended by Pople et al.[14] as implemented in Gaussian 03.[15] The choice of method and basis sets is based on a comparison with structural parameters obtained by X-ray analysis as well as model calculations done for the opening of the C4−C13 bond in **46** to **42** and the C6−C10 bond in **27** to **23** using HF, MP2, BP86, and B3LYP with various Pople basis sets. We found that using 3-21G or 6-31G* was sufficient for geometry optimizations and that 6-311G* was sufficient for single-point energy calculations. Thus, most of the geometry optimizations were performed at the B3LYP/3-21G or B3LYP/6-31G* level of theory, followed by a characterization of all stationary points as minima or first-order saddle points by harmonic vibrational frequency calculations. Energies were refined by single-point calculations with B3LYP/6-311G*. All data were corrected for the effect of zero-point energy, which were used unscaled.

To account for the effect of solvation, SCRF model calculations were performed for the ring closure of **42** to **46b** and of **23** to **27** using the polarizable continuum model (PCM).[16] They qualitatively revealed the same results but only small energy differences toward a slightly higher reaction enthalpy in both cases.

To rationalize the regioselectivity of the HCl addition to **31** and **32**, local reactivity descriptors based on the hard and soft acids and bases (HSAB) concept[17] were used. They can be derived from Parr's and Pearson's definition of the global softness, S,[18] and the local softness, s.[19]

$$S = \left(\frac{\partial N}{\partial \mu}\right)_{v(\vec{r})} \tag{1}$$

where N is the number of electrons, μ is the chemical potential, and $v(\vec{r})$ is the external potential. Local softness is defined as

$$s(\vec{r}) = \left(\frac{\partial \rho(\vec{r})}{\partial \mu}\right)_{v(\vec{r})} = \left(\frac{\partial \mu}{\partial v(\vec{r})}\right)_N S = f(\vec{r})S \tag{2}$$

where $\rho(\vec{r})$ is the electron density and $f(\vec{r})$ is the Fukui function

(5) Ritter, J.; Gleiter, R. *Liebigs Ann./Recl.* **1997**, 1179−1188.
(6) Behr, O. M.; Eglinton, G.; Galbraith, A. R.; Raphael, R. A. *J. Chem. Soc.* **1960**, 3614−3625.
(7) Sondheimer, F.; Pilling, G. M. *J. Am. Chem. Soc.* **1971**, *93*, 1970−1977.
(8) Zhou, Q.; Carroll, P. J.; Swager, T. M. *J. Org. Chem.* **1994**, *59*, 1294−1301.
(9) Hövermann, K. Ph.D. Dissertation, Universität Heidelberg, 1999.
(10) Schmidt, E. M.; Gleiter, R.; Rominger, F. *Chem.−Eur. J.* **2003**, *9*, 1814−1822.
(11) (a) Kohn, W.; Sham, L. J. *Phys. Rev. A: At., Mol., Opt. Phys.* **1965**, *140*, 1133−1138. (b) Parr, R. G.; Yang, W. *Density Functional Theory of Atoms and Molecules*; Oxford University Press: Oxford, U.K., 1989. (c) Koch, W.; Holthausen, M. C. *A Chemists Guide to Density Functional Theory*; Wiley-VCH: Weinheim, Germany, 2000.
(12) (a) Becke, A. D. *J. Chem. Phys.* **1992**, *96*, 2155−2160. (b) Becke, A. D. *J. Chem. Phys.* **1993**, *98*, 5648−5652. (c) Becke, A. D. *J. Chem. Phys.* **1993**, *98*, 1372−1377.
(13) (a) Lee, C.; Yang, W.; Parr, R. G. *Phys. Rev. B: Condens. Matter* **1988**, *37*, 785−789. (b) Stephens, P. J.; Devlin, F. J.; Chabalowski, C. F.; Frisch, M. J. *J. Phys. Chem.* **1994**, *98*, 11623−11627.
(14) Krishnan, K.; Binkley, J. S.; Seeger, R.; Pople, J. A. *J. Chem. Phys.* **1980**, *72*, 650−654.
(15) Frisch, M. J.; Trucks, G. W.; Schlegel, H. B.; Scuseria, G. E.; Robb, M. A.; Cheeseman, J. R.; Montgomery, J. A., Jr.; Vreven, T.; Kudin, K. N.; Burant, J. C.; Millam, J. M.; Iyengar, S. S.; Tomasi, J.; Barone, V.; Mennucci, B.; Cossi, M.; Scalmani, G.; Rega, N.; Petersson, G. A.; Nakatsuji, H.; Hada, M.; Ehara, M.; Toyota, K.; Fukuda, R.; Hasegawa, J.; Ishida, M.; Nakajima, T.; Honda, Y.; Kitao, O.; Nakai, H.; Klene, M.; Li, X.; Knox, J. E.; Hratchian, H. P.; Cross, J. B.; Bakken, V.; Adamo, C.; Jaramillo, J.; Gomperts, R.; Stratmann, R. E.; Yazyev, O.; Austin, A. J.; Cammi, R.; Pomelli, C.; Ochterski, J. W.; Ayala, P. Y.; Morokuma, K.; Voth, G. A.; Salvador, P.; Dannenberg, J. J.; Zakrzewski, V. G.; Dapprich, S.; Daniels, A. D.; Strain, M. C.; Farkas, O.; Malick, D. K.; Rabuck, A. D.; Raghavachari, K.; Foresman, J. B.; Ortiz, J. V.; Cui, Q.; Baboul, A. G.; Clifford, S.; Cioslowski, J.; Stefanov, B. B.; Liu, G.; Liashenko, A.; Piskorz, P.; Komaromi, I.; Martin, R. L.; Fox, D. J.; Keith, T.; Al-Laham, M. A.; Peng, C. Y.; Nanayakkara, A.; Challacombe, M.; Gill, P. M. W.; Johnson, B.; Chen, W.; Wong, M. W.; Gonzalez, C.; Pople, J. A. *Gaussian 03*, revision B.03; Gaussian, Inc.: Wallingford, CT, 2004.
(16) Miertus, S.; Scrocco, E.; Tomasi, J. *Chem. Phys.* **1981**, *55*, 117−129.
(17) (a) Pearson, R. G. *J. Am. Chem. Soc.* **1963**, *85*, 3533−3539. (b) Pearson, R. G.; Songstad, J. *J. Am. Chem. Soc.* **1967**, *89*, 1827−1836. (c) Pearson, R. G. *Surv. Prog. Chem.* **1969**, *5*, 1−52.
(18) Parr, R. G.; Pearson, R. G. *J. Am. Chem. Soc.* **1983**, *105*, 7512−7516.

SCHEME 3. Reduction of 10a with Sodium and the Reaction of 10b with Iodine

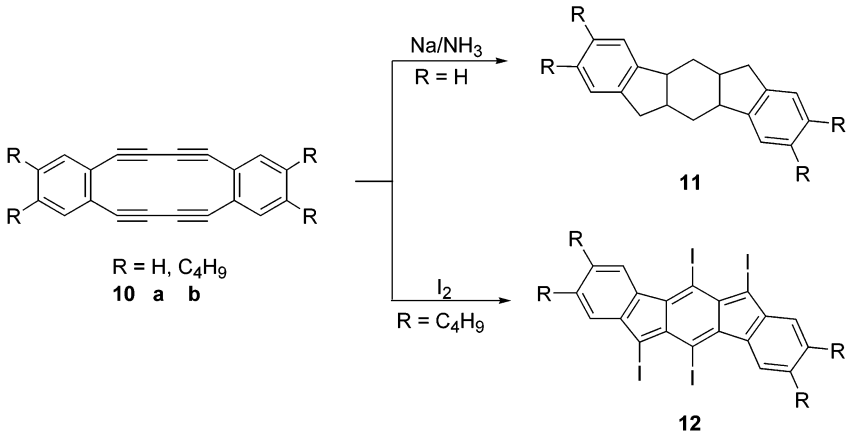

SCHEME 4. Experimental Results for the Addition of Hydrochloric Acid to 13b and 16b

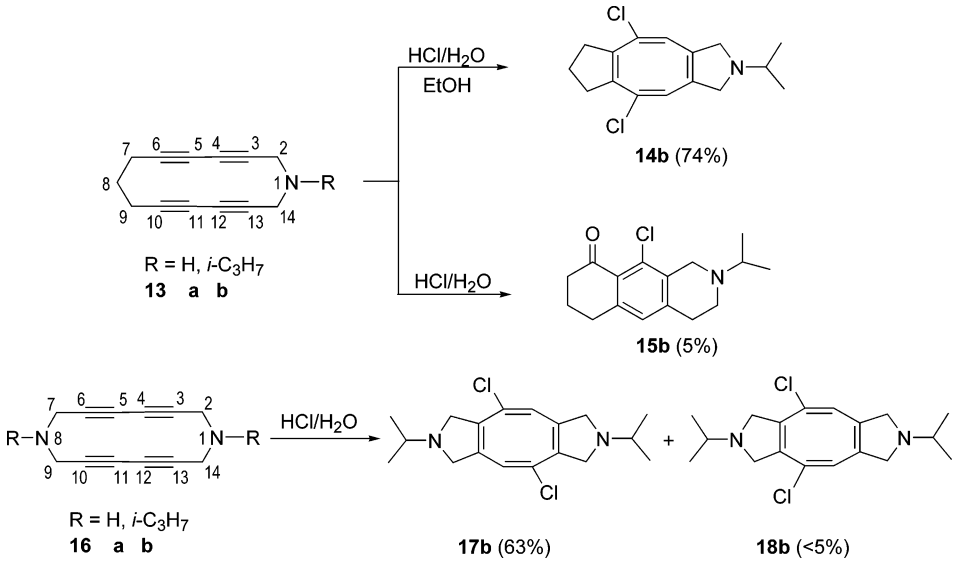

introduced by Parr Yang.[20] Both $s(\vec{r})$ and $f(\vec{r})$ can be used for studying intramolecular reactivity sequences.

The function $s(\vec{r})$ can be used to describe the reactivity of different molecules against a common reagent. It was shown by Yang and Mortier[21] that one can use three different local softness parameters using the electronic population on an atom **K** for the N_0, $N_0 + 1$, and $N_0 - 1$ electron systems ($\rho_K(N_0)$, $\rho_K(N_0 - 1)$ and $\rho_K(N_0 + 1)$).

$$s_K^+ = [\rho_K(N_0 + 1) - \rho_K(N_0)]S$$

$$s_K^- = [\rho_K(N_0) - \rho_K(N_0 - 1)]S$$

$$s_K^0 = \frac{1}{2}[\rho_K(N_0 + 1) - \rho_K(N_0 - 1)]S$$

It was shown[22] that the ratios s_K^-/s_K^+ and s_K^+/s_K^-, termed as "relative nucleophilicity" and "electrophilicity", respectively, are more reliable descriptors of intramolecular reactivity.

Results

(a) Proton Induced Ring Closure. To eludicate the reaction mechanism, we have carried out model calculations on the *N*-protonated parent systems **19** and **20** (Scheme 5). By replacing the *i*-propyl substituent by a hydrogen atom, we could omit conformational isomers arising from different possible conformations of the *i*-propyl group itself and from its axial or equatorial positioning. A protonation at the nitrogen atom seems very reasonable, for all of the reactions were carried out under very acidic conditions in either concentrated hydrochloric acid or a mixture of the latter with ethanol.

Treating these systems with concentrated HCl will yield the tricyclic systems **37** and **39** as main products in analogy to the reactions summarized in Scheme 4. Assuming a stepwise mechanism for the ring closure of **19** and **20**, various intermediates can be envisaged as summarized in Scheme 5. First, protonation occurs at C4 of the starting material (**19**, **20**), yielding the vinyl cations **21** and **22**, respectively. These cations undergo a ring closure between C3 and C13 as indicated by the arrows to give the bicyclic species **23** and **24**, respectively. A further transannular ring closure between C6 and C10 yields

(19) (a) Yang, W.; Parr, R. G. *Proc. Natl. Acad. Sci. U.S.A.* **1985**, *82*, 6723−6726. (b) Berkovitz, M.; Parr, R. G. *J. Chem. Phys.* **1988**, *88*, 2554−2557.

(20) Parr, R. G.; Yang, W. *J. Am. Chem. Soc.* **1984**, *106*, 4049−4050.

(21) Yang, W.; Mortier, W. J. *J. Am. Chem. Soc.* **1986**, *108*, 5708−5711.

(22) (a) Roy, R. K.; de Proft, F.; Geerlings, P. *J. Phys. Chem. A* **1998**, *102*, 7035−7040. (b) Roy, R. K.; Krishnamurti, S.; Geerlings, P.; Pal, S. *J. Phys. Chem. A* **1998**, *102*, 3746−3755.

SCHEME 5. Proposed Reaction Mechanism for the Addition of HCl to 19 and 20

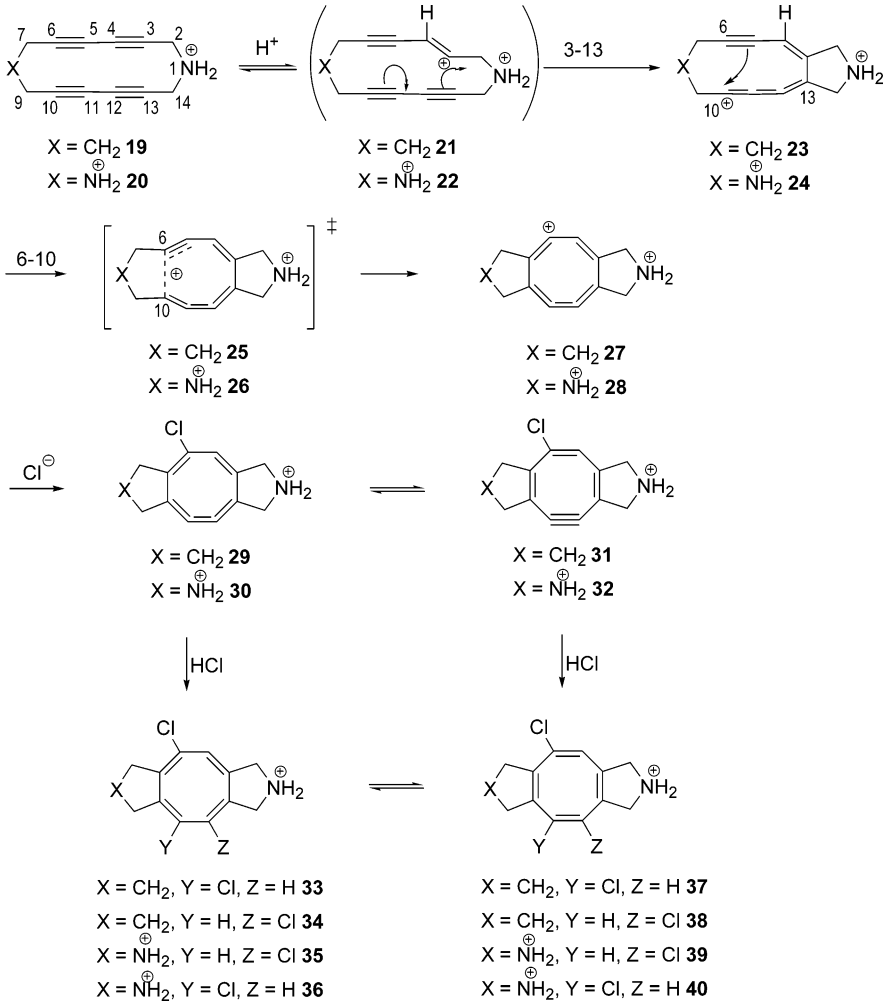

SCHEME 6. 41 as the Transition State between 21 and 42

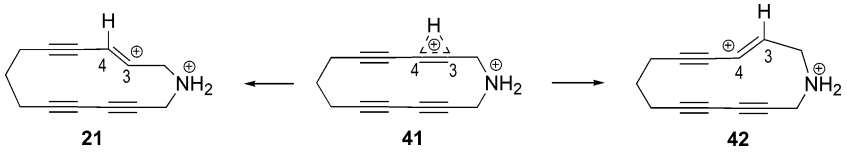

the tricyclic species **27** and **28** via the corresponding transition states **25** and **26** (Scheme 5).

The vinyl cations **27** and **28** can add a Cl^- to yield **29** and **30**, respectively. Furthermore, a valence isomerization to **31**/**32** is assumed before HCl adds to the highly strained triple bond, yielding the final products **37**/**39**. Another possibility leading to the latter would be addition of HCl to the central double bond of the butatriene system in **29**/**30** to **33**−**36**, followed by a valence isomerization to **37**−**40**.

The geometrical parameters of the possible intermediates listed in Scheme 5 were optimized. Apart from **21** and **22**, each of the postulated intermediates as well as the products could be located as minima on the potential energy surface. The optimized structures of the monoaza systems **19**−**38** are shown in Figure 1.

As input structure for **21** and **42**, was used the optimized structure of **19** with a proton bound to C4 or C3, respectively. These optimizations using B3LYP/3-21G yielded no minimum but converged to **23** and **24**, respectively. An input structure for **21** where the cationic carbon was bent away from the triple bond across the ring (C12−C13) led to **42** (Scheme 6) as minimum. To verify **21**, we also varied the basis set from 6-31G* to 6-31G** to 6−311++G** by using the DFT-(B3LYP) and HF methodology. All these efforts were in vain. This led us to conclude that **23** and **24** are the first intermediates following protonation of **19** and **20**, respectively (Scheme 5). In our search for the vinyl cationic intermediate **21**, we also explored the possibility of the presence of a flat minimum on the corresponding potential energy surface by starting with **23** and opening the C3−C13 bond. These efforts also showed no indication of **21** as a minimum.

A second approach to locate **21** began with the transition state **41**, resulting from protonation of **19** (Scheme 6). This transition state could be located at different levels of theory (B3LYP/3-21G, B3LYP/6-311++G**, HF/3-21G, and MP2/3-21G) and shows one imaginary frequency describing the oscillation of the proton between the positions 3 and 4 of **41**, of which **21** and **42** might be the corresponding minima.

CHART 1. Four Possible Products with Relative Energies (B3LYP/3-21G) Following the Protonation and Ring Closure of 19

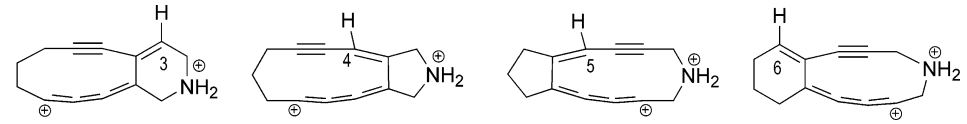

	46	**23**	**58**	**59**
E_{rel} (kcal/mol)	5.7	0.0	15.5	17.5

TABLE 1. Calculated Relative Energies (kcal/mol) and Most Relevant Distances for 23−28 (B3LYP/6-311G*), Including Imaginary Frequencies for 25 and 26

	rel. energy	C3−C4	C4−C5	C5−C6	C6−C10	C10−C11	C11−C12	C12−C13	C3−C13
23	14.6	1.36	1.40	1.21	3.17	1.24	1.29	1.31	1.46
25	22.4[a]	1.38	1.39	1.25	2.16	1.28	1.27	1.33	1.45
27	0.0	1.48	1.31	1.34	1.46	1.39	1.23	1.40	1.37
24	28.7	1.37	1.41	1.21	2.72	1.24	1.30	1.31	1.47
26	29.6[b]	1.38	1.40	1.23	2.31	1.26	1.28	1.32	1.46
28	0.0	1.49	1.31	1.34	1.44	1.37	1.23	1.40	1.38

[a] −368.1 cm^{-1}. [b] −246.7 cm^{-1}.

Starting from **41**, we carried out intrinsic reaction coordinate[23] calculations using B3LYP/3-21G to find a minimum along the reaction coordinate, which we assumed would lead to **21**. None of these calculations led to a minimum, but because of a steady decrease of the C3−C13 distance, they seem to directly approach **23**. This also points toward the nonexistence of **21**. Therefore, a concerted reaction of approaching the proton to C4 and closing the C3−C13 bond seems likely.

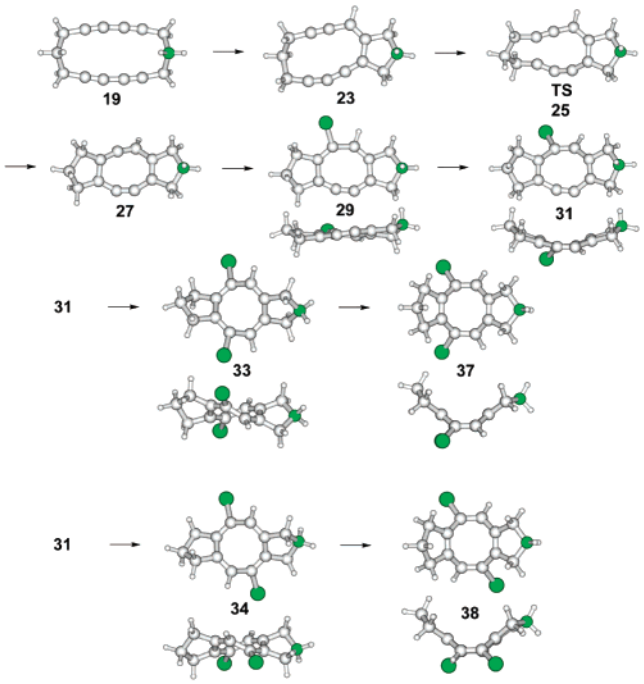

FIGURE 1. Optimized structures (B3LYP/6-311G* for **23**, **25**, and **27**; all others, B3LYP/6-31G*) of the monoaza systems **19**−**38**.

The process of protonation of **19** was examined for an attack to all four possible carbon atoms. **42** could be located as a minimum at the HF/3-21G, B3LYP/3-21G, and 6-311G* levels of theory. When a proton was added to C5 or C6 using HF/3-21G and 6-31G*, there could each be located a minimum representing the vinyl cations as analogous to **21** and **42**, but with B3LYP, the first minima to be found were **58** and **59**, respectively (see Chart 1).

The concerted motion of H−C4 and C3−C13 is also the outcome of a calculation in which both distances were varied independently. The resulting potential energy surface is shown in Figure 2. It becomes obvious that the energy of the system

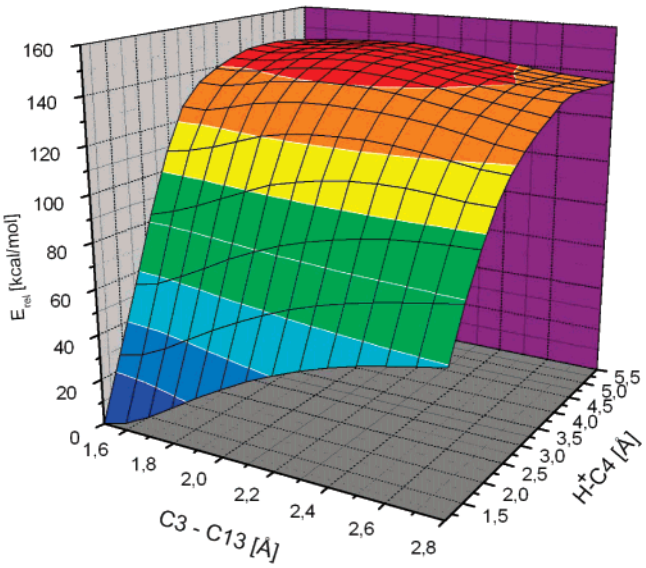

FIGURE 2. Potential Energy Surface for the Concerted Reaction of the Protonation and Cyclization of **19**−**23**.

is lowered with decreasing H−C4 distance. Below a H−C4 distance of about 3.5 Å, the closing of the C3−C13 bond is favored. At around 3.5 Å, the proton polarizes the electron density of the triple bond in such a way that a transannular ring closure occurs. For the ring closure of **20**, we assume the same mechanism.

The step that follows the concerted protonation and bond formation of **19** and **20** to **23** and **24**, respectively, is a second transannular ring closure to **27** and **28**. The corresponding transition states (**25**, **26**) could be located as first-order saddle points on the potential energy surface. The data listed in Table

(23) (a) Gonzalez, C.; Schlegel, H. B. *J. Phys. Chem.* **1990**, *94*, 5523−5527. (b) Fukui, K. *Acc. Chem. Res.* **1981**, *14*, 363−368.

SCHEME 7. Possible Intermediates and Products for the HCl Addition to 31 (top) and 32[a]

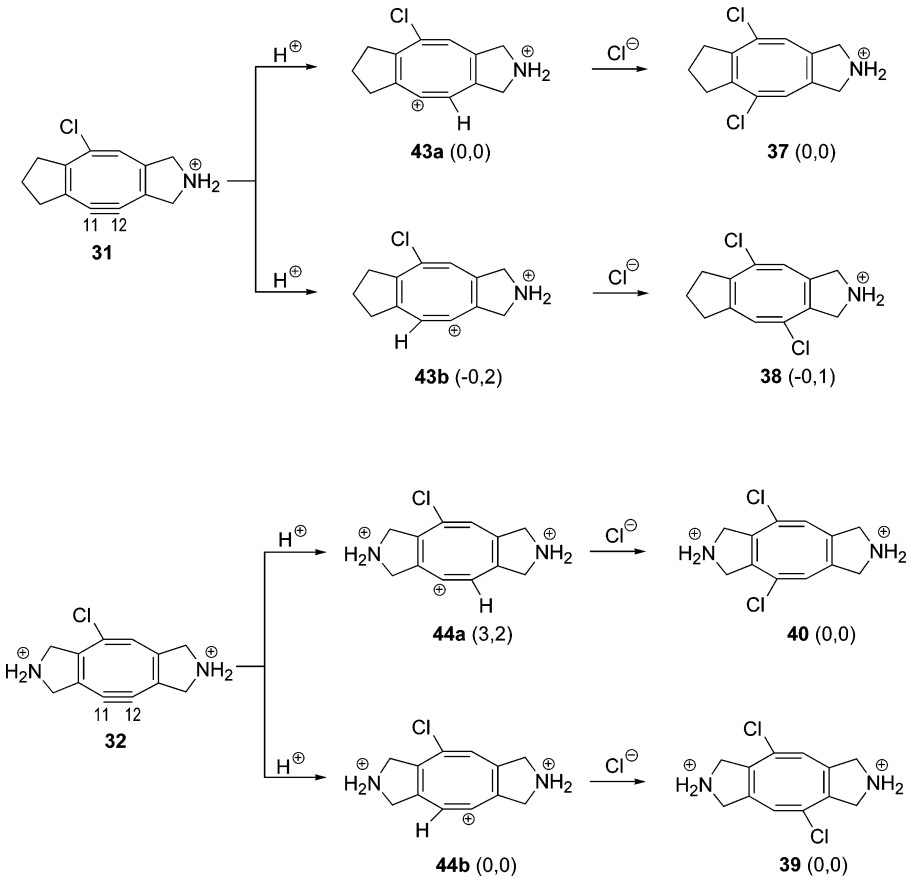

[a] Energy differences between isomers are given in brackets (B3LYP/6-31G*).

1 reveal that the second transannular bond (C6−C10) is closed with a rather low activation energy for **23** (7.8 kcal/mol) and **24** (0.9 kcal/mol). It was suggested recently[24] that B3LYP may systematically underestimate the stability of cyclic structures compared to that of acyclic ones. Therefore, test calculations with mPW1PW91/6-31G*[25] were performed on the ring closures of **23** and **24** to **27** and **28**, respectively. They revealed a higher exothermicity of 22.9 kcal/mol for the formation of **27** from **23** with a somewhat smaller activation energy of 4.6 kcal/mol. For **24**, no minimum could be located at all on this level of theory, correlating well with the B3LYP result of an almost vanishing activation energy for the ring closure to **28**.

The resulting intermediates **27** and **28** represent highly reactive vinyl cations. Therefore, stabilization by nucleophilic addition of a chloride anion yielding **29** and **30**, respectively, seems to be a reasonable assumption. Geometry optimization of the latter two species revealed twist-like conformations. No minimum could be found for a valence isomerized structure of **27** as analogues to **31**.

Two possibilities were explored for the further reaction of **29** and **30** to the final products **37**−**40**. The first route assumes a valence isomerization of **29** and **30** to **31** and **32** (Scheme 5) for which a boat conformation was calculated. The latter conformation is 6.1 kcal/mol (**31**) and 7.5 kcal/mol (**32**) more stable on the B3LYP/6-311G*//B3LYP/6-31G* level than the related twist-conformations (**29**, **30**). We refrained from locating transition states for these isomerizations because these steps of the reaction sequence did not seem as relevant for understanding the whole reaction process as the cyclization steps themselves.

The addition of a second equivalent of HCl to **31** and **32** yields **37**−**40**.

According to Scheme 5, we have explored a different route in which the second equivalent of HCl is added to the central double bond of the butatriene system in **29** and **30** yielding **33**−**36**. **33** and **35** still show a twist conformation and lie 5.1 kcal/mol (**33**) and 2.1 kcal/mol (**35**) above **37** and **39** as boat-shaped global minima. These data suggest that from **29**/**30** to **37**/**39** the path via **31**/**32** is the most favorable.

(b) Regioselectivity of the HCl Addition. As shown in Scheme 4, a regioselectivity in the addition of the second equivalent of hydrochloric acid is observed for **13b** and **16b**. Furthermore, a side reaction was reported for **13b**. This led to a 6−6−6 ring closure (**15b**) instead of the 5−8−5 ring closure to **14b**. To explain the regioselectivity of the HCl addition leading to the products, we at first optimized the geometries of the possible intermediates **43a**−**44b** and the final products **37**−**40** with respect to the total energy (Scheme 7). It turned out that the energy differences, each among the intermediates and products are too small to be significant (see Scheme 7). We, therefore, had to use specific descriptors for the nucleophilicity of a center. Instead of total energies, we apply the local softness parameters s_k^+ and s_k^- as well as the relative nucleophilicity s_K^-/s_K^+, as defined above. Our calculations are based on the

(24) Matsuda, S. P. T.; Wilson, W. K.; Xiong, Q. *Org. Biomol. Chem.* **2006**, *4*, 530−543.
(25) Adamo, C.; Barone, V. *J. Chem. Phys.* **1998**, *108*, 664−675.

SCHEME 8. Reaction Mechanism for the Generation of 51 from 19 and Hydrochloric Acid

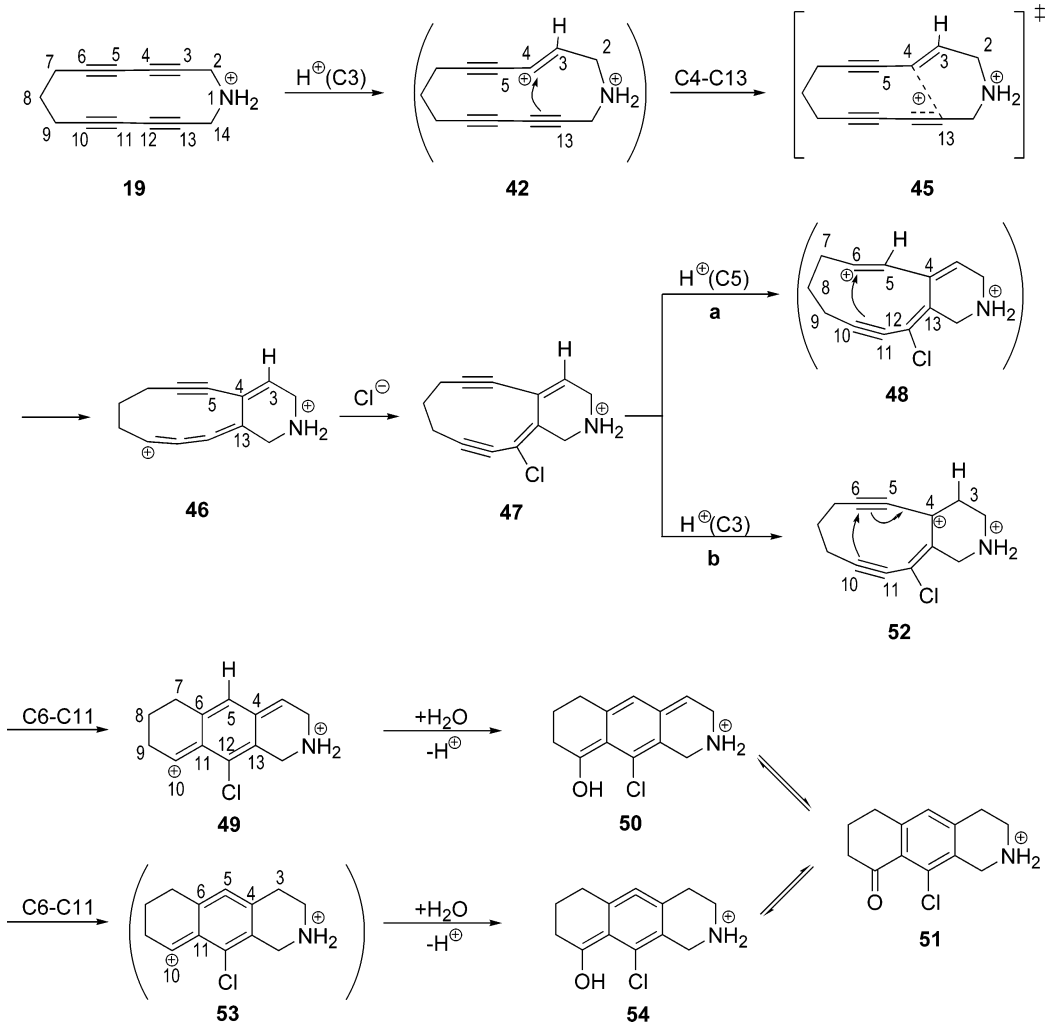

TABLE 2. Relative Nucleophilicities for C11 and C12 in 31 and 32

	basis set		C11	C12
31	6-311G*	s_K^-/s_K^+	0.893	1.219
	6-311+G**//6-31G*	s_K^-/s_K^+	0.378	0.939
32	6-311G*	s_K^-/s_K^+	1.217	1.120
	6-311+G**//6-31G*	s_K^-/s_K^+	1.108	0.914

geometrical parameters of **31** and **32** derived by B3LYP/6-31G* and B3LYP/6-311G*. When these geometries were used, single-point calculations were carried out for the species containing N_0 electrons, the radicals with $N_0 - 1$ electrons, and those with $N_0 + 1$ electrons, applying UB3LYP and the 6-311G* and 6-311+G** basis sets. The electronic populations (ρ_k) were calculated from Mulliken charges. The results for **31** and **32** are summarized in Table 2.

In the case of **31**, the highest relative nucleophilicity s_K^-/s_K^+ is predicted for C12, that is, a proton should prefer this position. In the case of the bisaza system **32**, the highest nucleophilicity is calculated for C11. These predictions agree with the experimentally observed regiochemistry for the second protonation step. It is interesting to note that for **31** the differences in s_K^-/s_K^+ for C11 and C12 are larger than for the bisaza system **32**. This result suggests that the addition to **32** should occur with a smaller degree of regioselectivity than to **31**. This outcome correlates very well with the experimental results showing no formation of **38**, but of both **39** (corresponding to **17b**) and to a smaller extent **40** (corresponding to **18b** in Scheme 4).

(c) Formation of a 6−6−6 Cycle. In Scheme 4, it is shown that the reaction of **13b** yielded a second tricyclic system, **15b**, containing three annulated six-membered rings. For the occurrence of this species, two possible mechanisms were proposed, as summarized in Scheme 8. Both start with a protonation of **19** at C3 yielding the vinyl cation **42**. This is followed by a transannular C4−C13 ring closure leading to the bicyclic **46** to which is added a chloride anion resulting in **47**. From **47** there are two possibilities, **a** and **b**: Protonation at C5 affords **48**, followed by ring closure between C6−C11 to the cation **49**, which is finally trapped by water to the enol **50**. The latter tautomerizes to the product **51**, the protonated parent system of **15b** (Scheme 4). In the second possible route, **47** is analogously protonated at C3, yielding the intermediates **52**, **53**, and **54**.

In contrast to **21** and **22**, the vinyl cation **42** could be located at some levels of theory. Optimizations at the B3LYP level with the basis sets 3-21G, 6-31G, 6-31G*, and 6-311G* as well as at HF level with the basis sets 3-21G and 6-31G* led to **42** as a more or less shallow minimum. The calculated barriers from **42** to the bicyclic vinyl cation **46** decrease from 6 kcal/mol (HF/3-21G) to 0.3 kcal/mol (B3LYP/6-311G*). Finally, at the MP2/

SCHEME 9. Addition of a Chloride Anion to 46 Yielding 47 or 47a

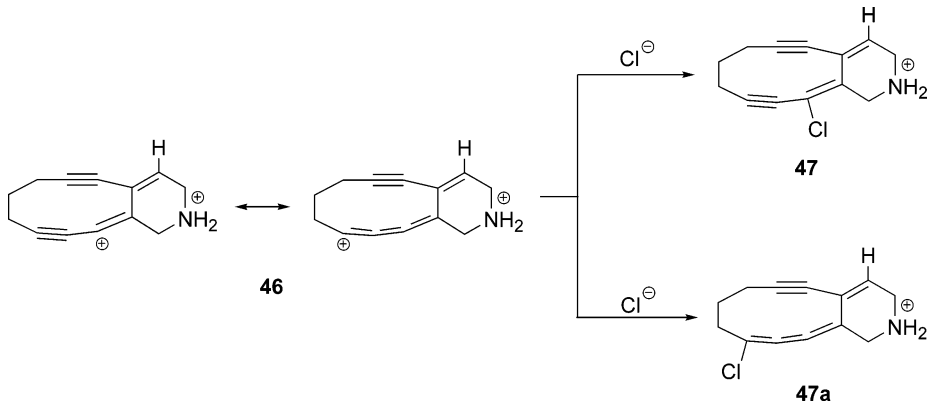

3-21G level of theory, no minimum is found for **42**. Due to these results for a barrier ranging from very small (B3LYP) to nonexisting (MP2), we assume that the protonation of **19** at C3 is accompanied by a C4−C13 ring closure in a concerted way, that is, **46** is the first intermediate. The optimized structures of **42**, **45**, and **46** are shown in Figure 3, and the most relevant calculated bond lengths of **46** are given in Table 3.

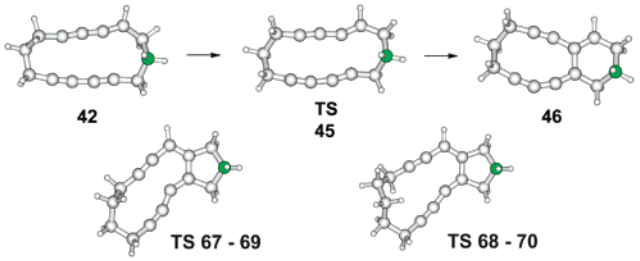

FIGURE 3. Optimized structures of **42**, **45**, and **46** (B3LYP/6-311G*) and of the transition states between **67**/**69** and **68**/**70** (B3LYP/6-31G*).

TABLE 3. Calculated Bond Lengths (Å) in 46, as Derived by B3LYP/6-311G*

C3−C4	C4−C5	C5−C6	C10−C11	C11−C12	C12−C13	C4−C13
1.35	1.42	1.21	1.25	1.20	1.31	1.52

These data suggest that the bicyclic system **46** is best described by the two valence structures, as shown in Scheme 9. The addition of a chloride anion thus leads to **47** or **47a** of which the latter is found (B3LYP/6-311G*//B3LYP/3-21G) to be 4.5 kcal/mol higher in energy than **47**.

Our calculations along the routes **a** and **b** (see Scheme 8) gave no evidence for the existence of the bicyclic vinyl cation **48**. The protonation of **47** at C5 is accompanied by a transannular ring closure yielding **49**. The intermediate **52** is predicted (B3LYP/6-311G*//B3LYP/3-21G) to be 21 kcal/mol above **49**, and the energy difference between **50** and **54** amounts to 52 kcal/mol in favor of the former. The postulated intermediate **53** does not exist as a minimum, but the second ring closure only occurs with the addition of a H_2O molecule. These results show that path **a** is more favorable than path **b**. Moreover, the calculations suggest, as discussed above, that the postulated intermediates **42**, **48**, and **53** do not exist as local minima on the potential energy surface. In the first two cases, protonation and transannular bond formation occur simultaneously.

In the ring-closure reaction of **19**, we have focused on the products **37** (Scheme 5) and **51** (Scheme 8) in analogy to the

CHART 2. Three Additional Possible Products that Would Result from a Protonation of 19 at C5 or C6

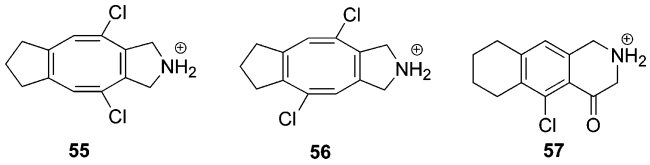

experimental results shown in Scheme 4. Besides **37** and **51**, there are three additional possible products, the isomers **55**−**57** listed in Chart 2. They can be derived by assuming an initial protonation of **19** at C5 or C6. As for **37** and **51**, each will be accompanied by a ring closure to a bicyclic system. In Chart 1, the relative energies obtained at the B3LYP/6-311G*//B3LYP/3-21G level of theory of the four possible bicyclic systems are compared. They are derived from a protonation at C3, C4, C5, or C6 and an accompanying transannular ring closure. The calculations reveal that **23** is the most stable one, followed by **46**. When the Bell−Evans−Polanyi principle is applied, the smallest activation energy is thus expected for the formation of **23** followed by **46**. These conclusions agree with the experimental results, as summarized in Scheme 4. For the order of stability of **23**, **46**, **58**, and **59**, the separation of the positive charges seems to take an influence.

(d) Extension to Rings with Two Nonparallel 1,3-Butadiyne Units. The two ring-closing processes, the proton-induced C3−C13 bond formation and the carbenium ion-induced C6−C10 bond formation of **19** and **20**, are facilitated by the close proximity (3.1 Å) of these centers.[10] When comparing this distance with the intermolecular CC distance of 1,3-butadiynes in the solid-state aligned parallel and inclined by 45° against the stacking axis, one finds values of 4.7−5.2 Å for the intermolecular distances between the C(sp) centers.[26,27] In these cases, a polymerization to an enyne product occurs with trans-configurated double bonds (Figure 4a). This polymerization is usually initiated by light, γ-rays, or heat.[28] The large distance of 4.7−5.2 Å between the alkyne units renders an induction by proton or Lewis acids less likely.[29] When the stacking axis of the 1,3-butadiyne units is close to 90°, the distance between the neighboring triple bonds reduces to 3.4−3.6 Å.[30] This distance is much closer to that found in **13b** and

(26) Wegner, G. *Z. Naturforsch., B: Chem. Sci.* **1969**, *24*, 824−832.
(27) Enkelmann, V. *Adv. Polym. Sci.* **1984**, *63*, 91−136.
(28) Sixl, H. *Adv. Polym. Sci.* **1984**, *63*, 49−90.
(29) Ouyang, X.; Fowler, F. W.; Lauher, J. W. *J. Am. Chem. Soc.* **2003**, *125*, 12400−12401.

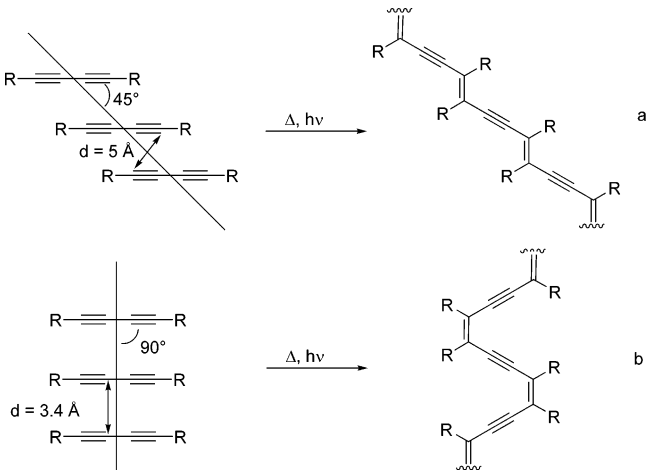

FIGURE 4. Diynepolymerization To Generate (a) a *trans*-Polybutadiyne and (b) a *cis*-Polybutadiyne.

SCHEME 10. Experimental Data for the Addition of HCl to 61

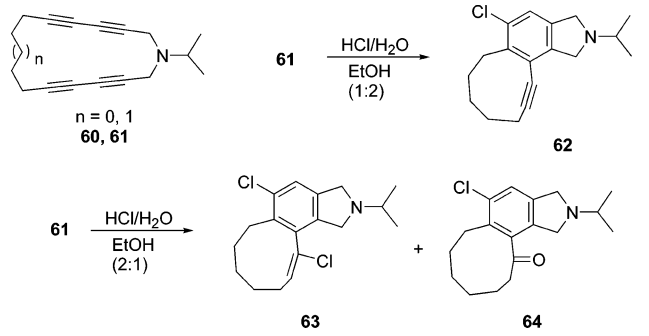

16b, and a proton-induced polymerization to a *cis*-enyne polymer (see Figure 4b) seems more likely. However, this kind of induction has not, in any of the cases, been tried experimentally.

These experiments and the results of the calculations presented above led us to carry out protonation experiments with cycles in which the two butadiyne units are not oriented in a parallel fashion. The compounds chosen were 1-isopropyl-1-aza cyclopentadeca-3,5,11,13-tetrayne (**60**) and 1-isopropyl-1-azacyclohexadeca-3,5,12,14-tetrayne (**61**).[31] For both species, a chairlike conformation is found, with the isopropyl group preferring the axial position and the tetra- and pentamethylene chains adopting zigzag-like arrangements. The transannular distances between the 1,3-butadiyne termini are 3.13 and 4.00 Å for **60** and 3.12 and 4.36 Å for **61**.[31] The geometrical parameters of both species could very well be reproduced at the B3LYP/6-31G* level of theory. The addition of hydrochloric acid to **61** as a representative example is summarized in Scheme 10. When the experiment is carried out with concentrated HCl in ethanol in a ratio of 1:2, only 1 equiv of HCl is added to yield **62**. When **61** was treated with concentrated HCl/EtOH in a ratio of 2:1, the compounds **63** and **64** were isolated.[31]

The quantum chemical calculations carried out on the protonation of **65** and **66** (Scheme 11) revealed that the protonation at C4 is accompanied by a transannular ring closure in a concerted way, yielding the bicyclic structures **67** and **68**.

SCHEME 11. Calculated Reaction Mechanism for the Addition of HCl to 65 and 66

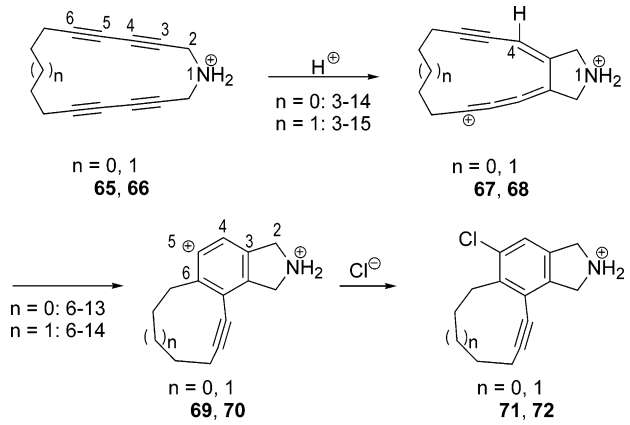

TABLE 4. Calculated Relative Energies (kcal/mol) for the Cyclization of 67 to 69 and 68 to 70[a]

	B3LYP/6-31G*	B3LYP/3-21G	B3LYP/6-311G*// B3LYP/6-31G*
67	9.8	4.4	6.8
TS	11.7 (−180.3)	7.0 (−225.4)	10.1
69	0.0	0.0	0.0
68[b]	11.8	6.1	9.1
TS	12.8 (−47.7)	9.0 (−201.0)	14.0
70	0.0	0.0	0.0

[a] The imaginary frequency for the corresponding transition state (cm^{-1}) is given in brackets. [b] The experimental X-ray conformation of the methylene chain was adopted for the starting geometry.

TABLE 5. Calculated Bond Distances of 67−70 and the Corresponding Transition States (B3LYP/6-31G*)

	C3−C4	C4−C5	C5−C6	C11−C12	C12−C13	C13−C14	C3−C14	C6−C13
67	1.36	1.40	1.22	1.25	1.30	1.32	1.46	3.47
TS	1.36	1.40	1.24	1.23	1.35	1.35	1.44	2.21
69	1.41	1.35	1.32	1.23	1.40	1.40	1.40	1.51
				C12−C13	C13−C14	C14−C15	C3−C15	C6−C14
68	1.36	1.40	1.22	1.25	1.30	1.32	1.46	3.53
TS	1.36	1.39	1.25	1.23	1.34	1.34	1.44	2.16
70	1.42	1.35	1.32	1.22	1.39	1.41	1.40	1.52

The activation energies for the C6−C13 and C6−C14 ring closure, respectively, to an aromatic unit are calculated to be 1.9 kcal/mol for **67** and 1.0 kcal/mol for **68** (B3LYP/6-31G*). The optimized structures of the corresponding transition states are shown in Figure 3. On the path from **67** to **69**, we noticed an additional local minimum due to a reorientation of the tetramethylene chain during the ring closure. In Table 4 are listed the calculated relative energies of **67**, **69**, **68**, **70** and the corresponding transition states. The most relevant calculated geometrical parameters are given in Table 5. The intermediates **69** and **70** will be stabilized to **71** and **72** by adding a chloride anion (Scheme 11).

Conclusion

Our first objective was to model the proton-induced ring closure of two parallel 1,3-butadiyne units held in close proximity in two 14-membered rings. These calculations revealed that an intermediate with a vinyl cationic unit pointing inside the ring does not exist on the potential energy surface.

(30) Coates, G. W.; Dunn, A. R.; Henling, L. M.; Dougherty. D. A.; Grubbs, R. H. *Angew. Chem.* **1997**, *109*, 290−293; *Angew. Chem., Int. Ed. Engl.* **1997**, *36*, 248−251.

(31) Schmidt, E. M.; Gleiter, R.; Rominger, F. *Eur. J. Org. Chem.* **2004**, 2818−2825.

The approach of a proton in the plane of the two 1,3-butadiyne units from outside is accompanied by a transannular ring closure in a concerted way. The calculations furthermore enabled us to rationalize the regioselectivity of the HCl addition to **31** and **32** by using Parr's and Pearson's local softness $s(\vec{r})$. The observed product selectivity is traced back to the relative stability of the primary protonation products. The stability of the dications **23**, **46**, **58**, and **59** correlates with the distance of the two cationic centers. In systems where the orientation of the two butadiyne units was not parallel anymore, the first step of protonation and ring closure to a bicyclic species also takes place in a concerted way. As a result of the larger distance of the other termini, a ring closure to an aromatic ring is preferred with a rather small activation energy.

Acknowledgment. We are grateful to the Deutsche Forschungsgemeinschaft for financial support. B.E. thanks the Studienstiftung des deutschen Volkes for a graduate fellowship.

Supporting Information Available: Tables listing electronic energies, Cartesian coordinates, and zero-point vibrationals for all the calculated species. This material is available free of charge via the Internet at http://pubs.acs.org.

JO060426H